Physics Letters B 728 (2014) 482–488

Contents lists available at ScienceDirect

Physics Letters B

www.elsevier.com/locate/physletb

Nuclear aspects of neutral current non-standard ν-nucleus reactions and the role of the exotic $\mu^- \to e^-$ transitions experimental limits

D.K. Papoulias, T.S. Kosmas *

Division of Theoretical Physics, University of Ioannina, GR 45100 Ioannina, Greece

ARTICLE INFO

Article history:
Received 10 September 2013
Received in revised form 24 October 2013
Accepted 8 December 2013
Available online 11 December 2013
Editor: J.-P. Blaizot

Keywords:
Lepton flavour violation
Mu-to-e conversion
Non-standard electroweak interactions
Quasi-particle RPA
Supernova neutrinos

ABSTRACT

The nuclear aspects of flavour changing neutral current (FCNC) processes, predicted by various new-physics models to occur in the presence of nuclei, are examined by computing the relevant nuclear matrix elements within the context of the quasi-particle RPA using realistic strong two-body forces. One of our aims is to explore the role of the non-standard interactions (NSI) in the leptonic sector and specifically: (i) in lepton flavour violating (LFV) processes involving the neutral particles ν_ℓ and $\tilde{\nu}_\ell$, $\ell = e, \mu, \tau$ and (ii) in charged lepton flavour violating (cLFV) processes involving the charged leptons ℓ^- or ℓ^+. As concrete nuclear systems we have chosen the stopping targets of $\mu^- \to e^-$ conversion experiments, i.e. the ^{48}Ti nucleus of the PRIME/PRISM experiment at J-PARC and the ^{27}Al of the COMET at J-PARC as well as of the Mu2e at Fermilab. These experiments have been designed to reduce the single event sensitivity down to 10^{-16}–10^{-18} in searching for charged lepton mixing events. Our goal is, by taking advantage of our detailed nuclear structure calculations and using the present limits or the sensitivity of the aforementioned exotic $\mu^- \to e^-$ experiments, to put stringent constraints on the parameters of NSI Lagrangians.

1. Introduction

In recent years, ongoing extremely sensitive experiments searching for physics beyond the current Standard Model (SM) expect to see new physics or to set severe limits on various physical observables and particle model parameters [1–3]. In particular, current experiments searching for flavour changing neutral current (FCNC) processes in the leptonic sector [3–9] may provide insights and new results into the physics of charged lepton flavour violation (cLFV) [7,8], neutrino oscillation in propagation [9] and others. The cLFV experiments, although they have not yet discovered any event, represent a very important probe to search for charged lepton mixing with significant implications on understanding various open issues in particle, nuclear physics and astrophysics [10–13]. To this purpose, exotic $\mu^- \to e^-$ conversion studies are interesting worldwide theoretically [14,15] as well as experimentally with two experiments: (i) the COMET at J-PARC, Japan [4], and (ii) the Mu2e at Fermilab, USA [5–7]. Both ambitious experiments expect to reach a single event sensitivity down to 10^{-16}–10^{-18}.

The best previous limit for the $\mu^- \to e^-$ conversion was obtained by the SINDRUM-II Collaboration at PSI on the reaction

$$\mu^- + {}^{48}\mathrm{Ti} \to e^- + {}^{48}\mathrm{Ti}, \tag{1}$$

as $R^{\mathrm{Ti}}_{\mu e} < 6.1 \times 10^{-13}$ [16] (many authors use the published upper limit $R^{\mathrm{Ti}}_{\mu e} < 4.3 \times 10^{-12}$ [17]), where $R^{\mathrm{Ti}}_{\mu e}$ denotes the branching ratio of the $\mu^- \to e^-$ conversion rate divided by the total μ^--capture rate in the ^{48}Ti nucleus. The COMET experiment, is expected to reach a high sensitivity, $R^{\mathrm{Al}}_{\mu e} < 10^{-16}$ [4] using ^{27}Al as muon-stopping target while the Mu2e experiment aims to improve $R^{\mathrm{Al}}_{\mu e}$ even further, i.e. to a single event sensitivity 2×10^{-17}, which with a background of 0.5 events will reach a target sensitivity $R^{\mathrm{Al}}_{\mu e} < 6 \times 10^{-17}$ [5–7]. The next decade experiments for cLFV, need very high intensity and quality muon beams, like those planed to be built at Fermilab for the Mu2e at Project-X and at J-PARC for the PRIME/PRISM experiments. The use of Project-X beams by the Mu2e experiment, expects to further decrease the upper bound to $R^{\mathrm{Al}}_{\mu e} < 2 \times 10^{-18}$ [18], while the PRIME experiment, based on the superior properties of the muon beam at J-PARC that can be delivered to the ^{48}Ti, may reach the sensitivity of $R^{\mathrm{Ti}}_{\mu e} < 10^{-18}$ [19,20].

We should mention the most stringent upper bounds on purely leptonic cLFV processes presently available for $\mu - e$ transitions, namely, the new limit on the branching ratio of the $\mu^+ \to e^+\gamma$ process, $Br(\mu^+ \to e^+\gamma) < 5.7 \times 10^{-13}$, set very recently by the MEG experiment at PSI using one of the most intense continuous

* Corresponding author.
E-mail addresses: dimpap@cc.uoi.gr (D.K. Papoulias), hkosmas@uoi.gr (T.S. Kosmas).

0370-2693
http://dx.doi.org/10.1016/j.physletb.2013.12.028

μ^+ beams in the world [21], and that of the $\mu \to eee$ process set previously by the SINDRUM II Collaboration in the value $Br(\mu^+ \to e^+e^+e^-) < 1.0 \times 10^{-12}$ [22].

In recent works, neutral current (NC) neutrino scattering processes on leptons, nucleons and nuclei involving interactions that go beyond the SM (non-standard interactions, NSI, for short) have been examined [10–12]. Such processes may be predicted from several extensions of the SM such as various realizations of the seesaw mechanism in the standard model [15,23,24] and left-right symmetric models [25]. The reactions of this type that take place in nuclei are represented by

$$\nu_\alpha(\tilde{\nu}_\alpha) + (A, Z) \to \nu_\beta(\tilde{\nu}_\beta) + (A, Z) \tag{2}$$

$(\alpha, \beta = e, \mu, \tau)$ and theoretically they can be studied under the same nuclear methods as the exotic cLFV process of $\mu^- \to e^-$ conversion in nuclei. Among the interesting applications of the reactions (2), those connected with the supernova physics may allow ν_e neutrinos to change flavour during core collapse creating ν_e neutrino holes in the electron-neutrino sea [26] which may allow e^--capture on nucleons and nuclei to occur and subsequently decrease the value of the electron fraction Y_e. Such non-standard interactions [27–29] may suggest alterations in the mechanisms of neutrino-propagation through the supernova (SN) envelope and affect constraints put on the physics beyond the SM as well as on some scenarios of supernova explosion [30–32]. This motivated the investigation of the NSI in both LFV and cLFV processes in solar and supernova environment [33,34] and motivated our present work too. Furthermore, the impact of non-standard neutrino interactions on SN physics was the main motivation of works examining their effect on supernova when the neutrino self-interaction is taken into account [13]. The extreme conditions under which neutrinos propagate after they are created in the SN core, may lead to strong matter effects. It is known that, in particular, the effect of small values of the NSI parameters can be dramatically enhanced in the inner strongly deleptonized regions [13].

In general, low-energy astrophysical and laboratory neutrino searches provide crucial information towards understanding the fundamental electroweak interactions, within and beyond the SM. Well-known astrophysical neutrino sources like the solar, supernova, Geoneutrinos, etc., constitute excellent probes in searching for a plethora of neutrino physics applications and new-physics open issues [35]. Since neutrinos interact extremely weakly with matter, they may travel astronomical distances and reach the Earth [36–38], etc. The recorded ν-signals in sensitive terrestrial nuclear detectors of low-energy neutrinos [39,40], could be simulated providing useful information relevant to the evolution of distant stars, the core collapse supernovae, explosive nucleosynthesis [41], neutrino oscillation effects and others. Recently it becames feasible to detect neutrinos by exploiting the NC interactions and measuring the nuclear recoil signal by employing detectors with very low-threshold energies [42,43]. The NC interactions, through their vector components can lead to an additive contribution (coherence) of all nucleons in the target nucleus [44–49].

The main purpose of the present Letter is to explore the nuclear physics aspects of the ν-nucleus reactions of Eq. (2) focusing on the role of the NSI which have not been studied in detail up to now. We should stress that, our strategy in studying the nuclear aspects of FCNC in nuclei, is to carry out realistic cross sections calculations for the exotic processes (1) and (2), including NSI terms in the relevant effective Lagrangian. The required nuclear matrix elements are evaluated within the context of the quasi-particle RPA, considering both coherent and incoherent processes by applying the advantageous state-by-state method developed in Refs. [33,50,51]. As a first step, we perform calculations for $gs \to gs$ transitions of the reactions (2) by solving the BCS equations, for even–even nuclear systems, and employing the experimental nuclear charge densities [52] for odd-A nuclei. For comparison of our results with those of other methods [11,12,26,44,45], SM cross sections calculations are also carried out. More specifically, our present results refer to the even–even ^{48}Ti isotope, the stopping target of SINDRUM II and PRIME/PRISM $\mu^- \to e^-$ experiments. We perform similar calculations for processes (2) in the ^{27}Al nucleus proposed as detector material in Mu2e and COMET experiments. Finally, we will use the experimental upper limits of the cLFV processes to put robust bounds on model parameters of the relevant Lagrangians and the ratios of the NSI contributions with respect to the SM ones.

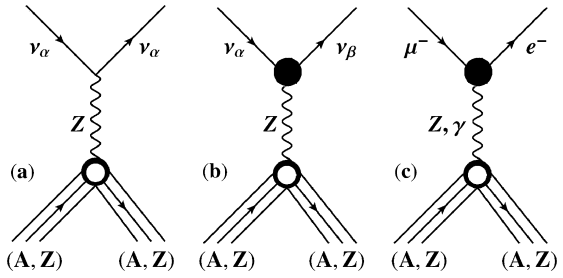

Fig. 1. Nuclear level Feynman diagrams for: (a) SM Z-exchange neutral current ν-nucleus reactions, (b) non-standard Z-exchange ν-nucleus reactions, and (c) Z-exchange and photon-exchange $\mu^- \to e^-$ in the presence of a nucleus (muon-to-electron conversion). The non-standard (cLFV or LFV) physics enters in the complicated vertex denoted by the bullet •.

2. Description of the formalism

The non-standard ν-nucleus processes (2) and the exotic cLFV $\mu^- \to e^-$ conversion in nuclei [1,14,15,34], can be predicted within the aforementioned new-physics models [15]. In Fig. 1 we show some nuclear-level Feynman diagrams representing the exchange of a Z-boson between a lepton and a nucleon for the cases of ν-nucleus scattering in the SM (Fig. 1(a)) and in the non-standard interactions of neutrinos with nuclei (Fig. 1(b)). We also show the exchange of a Z-boson or a γ-photon in the $\mu^- \to e^-$ conversion, Fig. 1(c) [14,15]. The leptonic vertex in the cases of Fig. 1(b), (c) is a complicated one. A general effective Lagrangian that involves SM interactions ($\mathcal{L}_{\rm SM}$) and NSI ($\mathcal{L}_{\rm NSI}$) with a non-universal (NU) term and a flavour changing (FC) term can be written as

$$\mathcal{L}_{\rm tot} = \mathcal{L}_{\rm SM} + \mathcal{L}_{\rm NSI} = \mathcal{L}_{\rm SM} + \mathcal{L}_{\rm NU} + \mathcal{L}_{\rm FC}. \tag{3}$$

The individual components $\mathcal{L}_{\rm SM}$ and $\mathcal{L}_{\rm NSI}$ of this Lagrangian are explained in the next subsections.

For a concrete example, it has been proposed [23] that, even small deviation from unitary lepton mixing matrix, may cause sizeable NSI effects and potentially large LFV [24]. The non-trivial structure of electroweak currents in low-scale seesaw Lagrangians leads to non-unitary lepton mixing matrix $N_{\alpha\beta}$, which can be parametrized as $N \equiv (1 - n)U$. $U_{\alpha\beta}$ is a unitary matrix and $n_{\alpha\beta}$ a model depended non-standard matrix $(\alpha, \beta = e, \mu, \tau)$ which takes specific form within seesaw mechanisms [24].

2.1. Non-standard ν-nucleus reaction cross sections

The neutral current non-standard neutrino interactions addressed here, are described by a quark-level Lagrangian, $\mathcal{L}_{\rm NSI}$, parametrized (for energies $\ll M_Z$) as [11,29,30]

$$\mathcal{L}_{\rm NSI} = -2\sqrt{2}G_F \sum_{\substack{f=u,d \\ \alpha,\beta=e,\mu,\tau}} \epsilon^{fP}_{\alpha\beta}[\bar{\nu}_\alpha \gamma_\rho L \nu_\beta]\big[\bar{f}\gamma^\rho P f\big], \tag{4}$$

where three light neutrinos ν_α with Majorana masses are considered, f denotes a first generation SM quark and $P = \{L, R\}$ are the chiral projectors. The Lagrangian (4) contains flavour preserving non-SM terms, known as non-universal (NU) interactions that are proportional to $\epsilon^{fP}_{\alpha\alpha}$, as well as flavour-changing (FC) terms proportional to $\epsilon^{fP}_{\alpha\beta}$, $\alpha \neq \beta$. These couplings are taken with respect to the strength of the Fermi coupling constant G_F [11,30]. For the polar-vector couplings we are mainly interested in the present work, it holds $\epsilon^{fV}_{\alpha\beta} = \epsilon^{fL}_{\alpha\beta} + \epsilon^{fR}_{\alpha\beta}$, while for the axial-vector couplings $\epsilon^{fA}_{\alpha\beta} = \epsilon^{fL}_{\alpha\beta} - \epsilon^{fR}_{\alpha\beta}$.

The nuclear physics aspects of the non-standard ν-matter reactions can be studied by transforming the Lagrangian (4) to the nuclear level where the hadronic current is written in terms of NC nucleon form factors (functions of the four momentum transfer) [34]. In the general case of the inelastic scattering of neutrinos on nuclei, the magnitude of the three momentum transfer, $q = |\mathbf{q}|$, obtained from the kinematics of the reaction, is a function of the scattering angle of the outgoing neutrino θ (laboratory frame), the initial, E_i, and final, E_f, neutrino energies, as well as the excitation energy of the target nucleus ω as, $q^2 = \omega^2 + 2E_iE_f(1-\cos\theta)$ [49,50]. In the special case of the coherent (elastic) channel we focus in this work ($\omega = 0$ and $E_i = E_f \equiv E_\nu$), only $gs \to gs$ transitions occur (for spin-zero nuclei) and we have $q^2 = 2E_\nu^2(1-\cos\theta)$ or $q = 2E_\nu \sin(\theta/2)$.

The coherent differential cross section with respect to the scattering angle θ for NSI ν-nucleus processes is written as

$$\frac{d\sigma_{\mathrm{NSI},\nu_\alpha}}{d\cos\theta} = \frac{G_F^2}{2\pi} E_\nu^2 (1+\cos\theta) \left|\langle gs| \left| G^{\mathrm{NSI}}_{V,\nu_\alpha}(q) \right| |gs\rangle\right|^2 \tag{5}$$

($\alpha = e, \mu, \tau$ denotes the flavour of incident neutrinos), where $|gs\rangle$ represents the nuclear ground state (for even–even nuclei, like the ^{48}Ti, $|gs\rangle = |J^\pi\rangle \equiv |0^+\rangle$). The nuclear matrix element, that arises from the Lagrangian (4), takes the form

$$\begin{aligned}\left|\mathcal{M}^{\mathrm{NSI}}_{V,\nu_\alpha}\right|^2 &\equiv \left|\langle gs| \left| G^{\mathrm{NSI}}_{V,\nu_\alpha}(q) \right| |gs\rangle\right|^2 \\ &= \left[\left(2\epsilon^{uV}_{\alpha\alpha} + \epsilon^{dV}_{\alpha\alpha}\right) Z F_Z(q^2) + \left(\epsilon^{uV}_{\alpha\alpha} + 2\epsilon^{dV}_{\alpha\alpha}\right) N F_N(q^2)\right]^2 \\ &\quad + \sum_{\beta\neq\alpha}\left[\left(2\epsilon^{uV}_{\alpha\beta} + \epsilon^{dV}_{\alpha\beta}\right) Z F_Z(q^2)\right. \\ &\quad \left. + \left(\epsilon^{uV}_{\alpha\beta} + 2\epsilon^{dV}_{\alpha\beta}\right) N F_N(q^2)\right]^2 \end{aligned} \tag{6}$$

($\beta = e, \mu, \tau$), where $F_{Z(N)}$ denote the nuclear (electromagnetic) form factors for protons (neutrons) entered due to the CVC theory. We note that in the adopted NSI model, the coherent NC ν-nucleus reaction is not a flavour blind process. By considering the nuclear structure details, the cross sections provided by Eq. (5), become more realistic and accurate [29] (in Ref. [11] the variation versus the momentum transfer of the nuclear form factor is neglected, which for supernova neutrino studies is a rather crude approximation [53]).

From an experimental physics point of view, many neutrino detectors are more sensitive to the recoil energy of the nuclear target, T_N, than to the scattering angles, θ. Therefore, it is also important to compute the differential cross sections $d\sigma/dT_N$. For coherent scattering the nucleus recoils (intrinsically it remains unchanged) with energy which, in the approximation $T_N \ll E_\nu$ (low-energy limit), is maximized as, $T_N^{\max} = 2E_\nu^2/(M + 2E_\nu)$, with M being the nuclear mass [47,48]. Then, to a good approximation, the square of the three momentum transfer, is equal to $q^2 = 2MT_N$, and the coherent NSI differential cross section with respect to T_N is written as

$$\frac{d\sigma_{\mathrm{NSI},\nu_\alpha}}{dT_N} = \frac{G_F^2 M}{\pi}\left(1 - \frac{MT_N}{2E_\nu^2}\right)\left|\langle gs| \left| G^{\mathrm{NSI}}_{V,\nu_\alpha}(q) \right| |gs\rangle\right|^2. \tag{7}$$

Both Eqs. (5) and (7) are useful for studying the nuclear physics of NSI of neutrinos with matter.

Furthermore, by performing numerical integrations in Eq. (5) over the scattering angle θ or in Eq. (7) over the recoil energy T_N, one can obtain integrated (total) coherent NSI cross sections, $\sigma_{\mathrm{NSI},\nu_\alpha}$. The individual cross sections $\sigma_{\mathrm{NU},\nu_\alpha}$ and $\sigma_{\mathrm{FC},\nu_\alpha}$ may be evaluated accordingly [53].

2.2. SM coherent ν-nucleus cross sections

At low and intermediate neutrino energies considered in this Letter, the effective (quark-level) SM ν-nucleus interaction Lagrangian, $\mathcal{L}_{\mathrm{SM}}$, reads

$$\mathcal{L}_{\mathrm{SM}} = -2\sqrt{2}G_F \sum_{\substack{f=u,d\\ \alpha=e,\mu,\tau}} g_P^f \left[\bar{\nu}_\alpha \gamma_\rho L \nu_\alpha\right]\left[\bar{f}\gamma^\rho P f\right], \tag{8}$$

where g_f^P are the P-handed SM couplings of f-quarks ($f = u, d$) to the Z-boson. We mention that, compared to previous studies [12,26], we have taken into consideration the $\nu - u$ quark interaction [see Eq. (6)], in addition to the momentum dependence of the nuclear form factors.

For coherent ν-nucleus scattering, the SM angle-differential cross section is given from an expression similar to Eq. (5) with the nuclear matrix element being that of the Coulomb operator $\hat{\mathcal{M}}_0(q)$ (product of the zero-order spherical Bessel function times the zero-order spherical harmonic [49]). This corresponding matrix element can be cast in the form [33]

$$\begin{aligned}\left|\mathcal{M}^{\mathrm{SM}}_{V,\nu_\alpha}\right|^2 &\equiv \left|\langle gs||\hat{\mathcal{M}}_0||gs\rangle\right|^2 \\ &= \left[g_V^p Z F_Z(q^2) + g_V^n N F_N(q^2)\right]^2, \end{aligned} \tag{9}$$

where $g_V^{p(n)}$ is the known polar-vector coupling of proton (neutron) to the Z boson (see Fig. 1(a)). In the low energy limit, one can also write in a straightforward manner the corresponding differential cross section with respect to the nuclear recoil energy, T_N [47,48]. In this work, starting from original differential cross sections $d\sigma_{\lambda,\nu_\alpha}/d\cos\theta$ and $d\sigma_{\lambda,\nu_\alpha}/dT_N$, we evaluated individual angle-integrated cross sections of the form $\sigma_{\lambda,\nu_\alpha}(E_\nu)$, with $\alpha = e, \mu, \tau$, and $\lambda = \mathrm{tot}, \mathrm{SM}, \mathrm{NU}, \mathrm{FP}, \mathrm{FC}$, where under FC, the six processes $\nu_e \leftrightarrow \nu_\mu$, $\nu_e \leftrightarrow \nu_\tau$, $\nu_\mu \leftrightarrow \nu_\tau$ are included (obviously, $\sigma_{\nu_\alpha\to\nu_\beta} = \sigma_{\nu_\beta\to\nu_\alpha}$) for both nuclei, ^{48}Ti and ^{27}Al. A great part of these results is presented and used to compute folded cross sections below (for more results see Ref. [53]).

3. Results and discussion

3.1. Nuclear structure calculations

At first, we studied the nuclear structure details of the matrix elements entering Eqs. (5)–(7) and Eq. (9) that reflect the dependence of the coherent cross section on the incident ν-energy E_ν and the scattering angle θ (or the recoil energy T_N). For the even–even ^{48}Ti nucleus, the stopping target of the PSI [16,17] and PRIME [19,20] experiments, this study involves realistic nuclear structure calculations for the cross sections $d\sigma_{\lambda,\nu_\alpha}/d\cos\theta$ and $d\sigma_{\lambda,\nu_\alpha}/dT_N$, performed after constructing the nuclear ground state $|gs\rangle$ by solving iteratively the BCS equations [50]. Then, the nuclear form factors for protons (neutrons) are obtained as [33]

$$F_{N_n}(q^2) = \frac{1}{N_n}\sum_j [j]\langle j|j_0(qr)|j\rangle \left(\upsilon^j_{N_n}\right)^2 \tag{10}$$

with $[j] = \sqrt{2j+1}$, $N_n = Z$ (or N). $\upsilon^j_{N_n}$ denotes the occupation probability amplitude of the j-th single nucleon level. The cho-

Table 1
The ratios R_{λ,ν_α} (for the definition see Eq. (12) in the text) of all possible $\nu_\alpha + (A,Z) \to \nu_\beta + (A,Z)$ processes. They have been evaluated in their asymptotic values reached at $E_\nu \approx 120$ MeV.

ν_α	(A,Z)	$R_{\rm tot}$	$R_{\rm NU}$	$R_{\rm FP}$	$R_{\nu_\alpha \leftrightarrow \nu_e}$	$R_{\nu_\alpha \leftrightarrow \nu_\mu}$	$R_{\nu_\alpha \leftrightarrow \nu_\tau}$
ν_e	^{48}Ti	1.037	0.002	0.905	–	0.121×10^{-4}	0.130
	^{27}Al	1.044	0.003	0.902	–	0.130×10^{-4}	0.139
ν_μ	^{48}Ti	1.293	0.001	0.929	0.121×10^{-4}	–	0.361
	^{27}Al	1.318	0.001	0.927	0.130×10^{-4}	–	0.387

sen active model space consists of the lowest 15 single-particle j-orbits, $j \equiv (n,\ell,1/2)j$ without core, up to major h.o. quanta $N = 4\hbar\omega$. The required monopole (pairing) residual interaction, obtained from a Bonn C–D two-body potential was slightly renormalized with the two parameters $g^{p,n}_{\rm pair}$ ($g^{p}_{\rm pair} = 1.056$, for proton pairs, and $g^{n}_{\rm pair} = 0.999$, for neutron pairs).

We note that, we have devoted a special effort on the accurate construction of the nuclear ground state, (i) because the coherent channel is the dominant one for the neutral current SM ν-nucleus processes and we assumed that this holds also for NSI processes, and (ii) because in a next step we are intended to perform extensive incoherent cross sections calculations where all accessible final nuclear states will be built on the present ground state.

For the odd-A ^{27}Al nucleus (its ground state spin is $|gs\rangle = |J^\pi\rangle = |(5/2)^+\rangle$), the stopping target of Mu2e and COMET experiments, we obtained the form factor $F_Z(q^2)$, through a model independent analysis (using a Fourier–Bessel expansion model) of the electron scattering data for the charge density distribution of this isotope [52]. Since similar data for $F_N(q^2)$ ^{27}Al are not available, we considered (to a rather satisfactory approximation) that $F_N \simeq F_Z$ (a difference up to about 10% usually appears for medium and heavy nuclear systems [52]). The momentum dependence of the nuclear form factors was ignored by some authors [11] which at low ν-energies relevant for solar neutrinos is practically a good approximation, but for energies relevant to supernova neutrinos addressed in this work, it may lead to differences of even an order of magnitude [53].

3.2. Integrated coherent ν-nucleus cross sections

In the next step of our calculational procedure we obtained angle-integrated coherent ν-nucleus cross sections by integrating numerically Eq. (5) over angles [or Eq. (7) over T_N] for the various interaction components as

$$\sigma_{\lambda,\nu_\alpha}(E_\nu) = \int \frac{d\sigma_{\lambda,\nu_\alpha}}{d\cos\theta}(\theta, E_\nu)\, d\cos\theta \tag{11}$$

($\lambda = {\rm tot, SM, NU, FP, FC}$). We found that the exotic FCNC processes $\nu_\alpha \to \nu_\beta$ in ^{48}Ti have significantly lower cross section compared to the SM one. From the obtained FCNC ν-nucleus cross sections the most challenging result corresponds to the $\nu_\mu \to \nu_e$ transition (and to its lepton conjugate process, $\nu_e \to \nu_\mu$). This is mainly due to the severe constraint $\epsilon^{fP}_{\mu e} = 2.9 \times 10^{-4}$ inserted in the Lagrangian (4) which has been derived from the nuclear $\mu^- \to e^-$ conversion experimental limits on cLFV branching ratio [4–7]. We remind that, in this work we have employed the NSI parameters $\epsilon^{fV}_{\alpha\beta}$ (except the $\epsilon^{fV}_{\mu e}$) derived from various experimental bounds in Ref. [10].

By exploiting our cross sections $\sigma_{\lambda,\nu_\alpha}(E_\nu)$, we find it interesting to estimate the ratio of each of the individual cross sections, $\sigma_{\lambda,\nu_\alpha}$, with respect to the SM cross sections defined as

$$R_{\lambda,\nu_\alpha}(E_\nu) = \frac{\sigma_{\lambda,\nu_\alpha}(E_\nu)}{\sigma_{\rm SM}(E_\nu)}, \quad \lambda = {\rm tot, NU, FP, FC}. \tag{12}$$

For ^{48}Ti, the latter ratios initially are slowly increasing functions of E_ν, but eventually (for energies higher than about 80–120 MeV) they tend asymptotically to the values listed in Table 1. For ^{27}Al, however, the ratios R_{λ,ν_α} are energy independent which is a consequence of the different treatment applied in studying the nuclear structure details than that followed for ^{48}Ti. From the comparison of the results of Table 2 with those of the method [11], we conclude that our realistic calculations are important in the case of ^{48}Ti nucleus, where the BCS method gave us $F_N \neq F_Z$ and, hence, the results obtained for R_{λ,ν_α} differ from those given by Ref. [11]. For ^{27}Al, however, for which we considered $F_N \simeq F_Z$, the dependence on the nuclear structure parameters in the numerator and denominator of Eq. (12) cancel out and, then, our predictions for R_{λ,ν_α} are equal to those of Ref. [11].

It is worth noting that, some constraints coming from solar [27] and atmospheric [28] neutrino data indicate that the NSI might be large, while according to the present experimental data, $\epsilon^{fV}_{\tau\tau}$ is unacceptably large and, consequently, it derives unrealistic results (the corresponding FP and NU cross sections, not included here, are larger than the SM ones) [10,29].

3.3. Supernova neutrino fluxes and expected event rates

One of the most interesting connections of our present calculations with ongoing and future neutrino experiments is related to supernova ν-detection. As it is known, in SN explosions most of the energy is released by ν-emission. Then, the total neutrino flux, $\Phi(E_\nu)$, arriving at a terrestrial detector reads [44,45]

$$\Phi(E_\nu) = \sum_\alpha \Phi_{\nu_\alpha}(E_\nu) = \sum_\alpha \frac{N_{\nu_\alpha}}{4\pi d^2}\eta^{\rm SN}_{\nu_\alpha}(E_\nu) \tag{13}$$

($\alpha = e,\mu,\tau$), where N_{ν_α} is the number of (anti)neutrinos emitted from a supernova source at a typical distance (here we used $d = 8.5$ kpc) and $\eta^{\rm SN}_{\nu_\alpha}$ denotes the energy distribution of the (anti)neutrino flavour α [47]. We assume that the emitted SN-neutrino energy spectra $\eta^{\rm SN}_{\nu_\alpha}(E_\nu)$ resemble Maxwell–Boltzmann distributions that depend on the temperature T_{ν_α} of the (anti)neutrino flavour ν_α ($\tilde\nu_\alpha$). By convoluting the integrated cross section $\sigma_{\lambda,\nu_\alpha}(E_\nu)$ with the neutrino distributions, the signal produced on a terrestrial detector may be simulated as

$$\sigma^{sign}_{\lambda,\nu_\alpha}(E_\nu) = \sigma_{\lambda,\nu_\alpha}(E_\nu)\eta^{\rm SN}_{\nu_\alpha}(E_\nu). \tag{14}$$

The resulting signals, $\sigma^{sign}_{\lambda,\nu_\alpha}(E_\nu)$, obtained by inserting in Eq. (14) the cross sections $\sigma_{\lambda,\nu_\alpha}$, are plotted in Fig. 2. Note that, in contrast to the original cross sections, now $\sigma^{sign}_{\nu_\alpha\to\nu_\beta} \neq \sigma^{sign}_{\nu_\beta\to\nu_\alpha}$. Fig. 2 shows that for incoming ν_μ neutrinos the signal $\sigma^{sign}_{\lambda,\nu_\mu}$ presents an appreciably wider energy range compared to that of ν_e and that the maximum peak is shifted towards higher energies following the features of the distributions $\eta^{\rm SN}_{\nu_\alpha}(E_\nu)$. The simulated cross sections of Fig. 2 reflect the characteristics of the incident neutrino spectrum of a specific flavour α having its own position of the maximum peak and width of the distribution $\eta^{\rm SN}_{\nu_\alpha}$. We remind that, as usually, for incoming ν_e neutrinos, the distribution $(\eta^{\rm SN}_{\nu_e} + \eta^{\rm SN}_{\tilde\nu_e})/2$ is used.

Table 2
Flux averaged cross sections $\langle\sigma_{\lambda,\nu_\alpha}\rangle$ (in 10^{-40} cm^2) for various supernova neutrino spectra parametrized by Maxwell–Boltzmann distributions.

ν_α	(A, Z)	$\langle\sigma_{\rm tot}\rangle$	$\langle\sigma_{\rm SM}\rangle$	$\langle\sigma_{\rm NU}\rangle$	$\langle\sigma_{\rm FP}\rangle$	$\langle\sigma_{\nu_\alpha\to\nu_e}\rangle$	$\langle\sigma_{\nu_\alpha\to\nu_\mu}\rangle$	$\langle\sigma_{\nu_\alpha\to\nu_\tau}\rangle$
ν_e	^{48}Ti	5.32	5.15	1.20×10^{-2}	4.66	–	6.07×10^{-5}	6.50×10^{-1}
	^{27}Al	1.57	1.50	3.83×10^{-3}	1.35	–	1.95×10^{-5}	2.09×10^{-1}
ν_μ	^{48}Ti	19.6	15.2	1.93×10^{-2}	14.2	1.80×10^{-4}	–	5.36
	^{27}Al	6.07	4.61	6.42×10^{-3}	4.27	6.00×10^{-5}	–	1.78

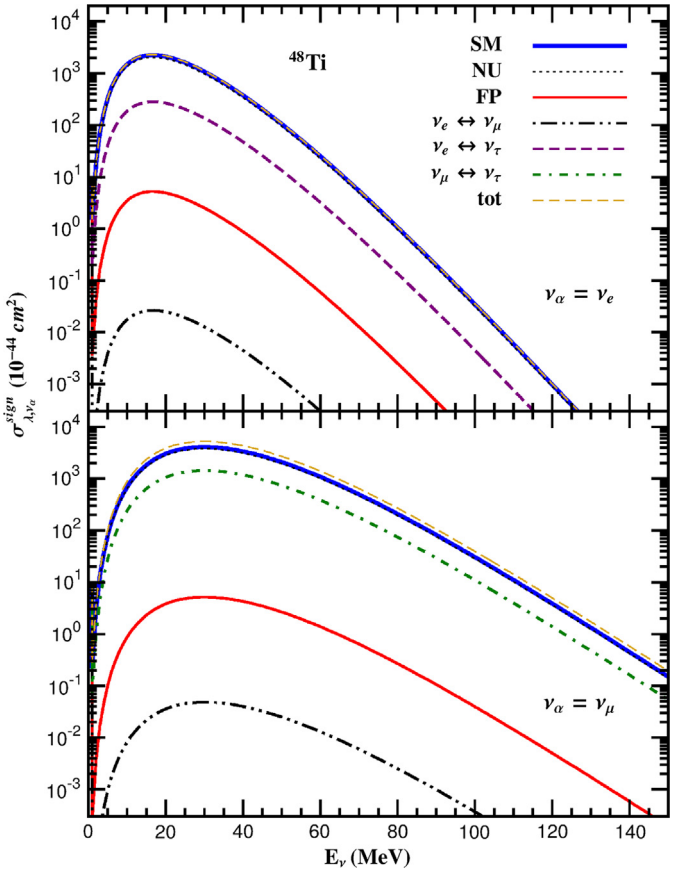

Fig. 2. The convoluted cross sections, evaluated with Maxwell–Boltzmann distributions, that represent the expected signal to be recorded on ^{48}Ti ν-detector, $\sigma^{sign}_{\lambda,\nu_\alpha}(E_\nu)$. Due to the flavour dependence of the SN neutrino distribution, the energy-window of ν_e neutrinos signal is more narrow compared to those of ν_μ and ν_τ neutrinos.

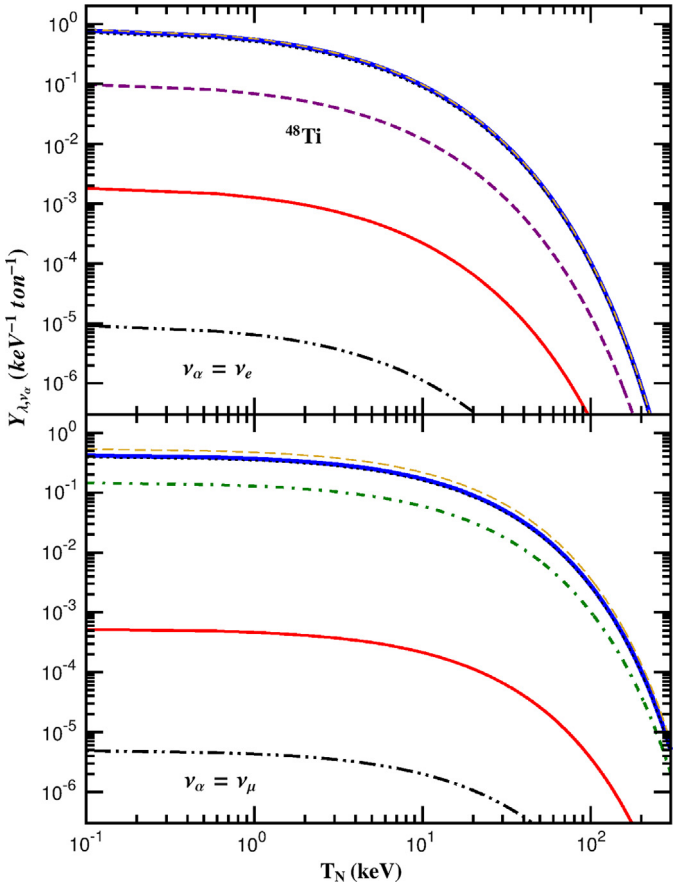

Fig. 3. Differential event rate, $Y_{\lambda,\nu_\alpha}(T_N)$, as a function of the nuclear recoil energy, T_N, for ^{48}Ti ν-detector. The line labelling is same to that of Fig. 2.

In SN neutrino simulations, another useful quantity is the flux averaged cross section [35] which in our notation is written as

$$\langle\sigma_{\lambda,\nu_\alpha}\rangle = \int \sigma_{\lambda,\nu_\alpha}(E_\nu)\eta^{\rm SN}_{\nu_\alpha}(E_\nu)\,dE_\nu. \tag{15}$$

The results for $\langle\sigma_{\lambda,\nu_\alpha}\rangle$, obtained by using our angle-integrated cross sections are listed in Table 2. We note that our flux averaged cross sections differ by about 30% from those of [11].

From experimental physics perspectives, it is also interesting to make predictions for the differential event rate of a ν-detector [44,45,51]. The usual expression for computing the yield in events is based on the neutrino flux, Φ_{ν_α}. To include the NSI of neutrinos with nuclei, the yield in events $Y_{\lambda,\nu_\alpha}(T_N)$, is [44,45]

$$Y_{\lambda,\nu_\alpha}(T_N) = N_t \int \Phi_{\nu_\alpha}\,dE_\nu \int \frac{d\sigma_{\lambda,\nu_\alpha}}{d\cos\theta}\delta\left(T_N - \frac{q^2}{2M}\right)d\cos\theta, \tag{16}$$

where N_t is the total number of nuclei in the detector material. Assuming a detector filled with one tone ^{48}Ti, we evaluated differential event rates $Y_{\lambda,\nu_\alpha}(T_N)$ for several supernova scenarios. These results are plotted in Fig. 3 where for each particular interaction, the corresponding neutrino flux has been considered. We see that, the respective results for the NU and FC processes, especially the case of $\nu_\mu \to \nu_e$ transition, present appreciably small contributions and that, the lower the energy recoil, the larger the potentially detected number of events. Hence, for the observation of non-standard ν-nucleus events, detector medium with very low energy-recoil threshold is required.

With the above results for $Y_{\lambda,\nu_\alpha}(T_N)$, one can obtain the total number of counts by integrating Eq. (16) above the energy threshold, $T_N^{thres.}$, of the detector in question. For the ^{48}Ti nucleus, assuming $T_N^{thres.} \approx 1$ keV, we find about 13.5 events/ton for the SM process but only 10^{-3} events/ton for the flavour changing $\nu_\mu \leftrightarrow \nu_e$ reaction, i.e. about four orders of magnitude less events [53]. We also conclude that, for making accurate predictions of the total number of counts, the nuclear structure parameters play significant role. Thus, for the $\nu_\mu \to \nu_e$ transition we end up with about 29% less events, compared to those given by the approximation of Ref. [11]. On the other hand, adding up the total number of events for the three SM processes of the form, $\nu_\alpha \to \nu_\alpha$, we end up with

Table 3
Upper limits on the NSI parameters $\epsilon_{\mu e}^{fV}$ and the ratios $R_{\nu_\mu \leftrightarrow \nu_e}$ for the FC $\nu_\mu \leftrightarrow \nu_e$ reaction channel resulting from the sensitivity of the $\mu^- \to e^-$ conversion experiments.

Parameter	COMET	Mu2e	Project-X	PRIME
$\epsilon_{\mu e}^{fV} \times 10^{-6}$	3.70	2.87	0.52	0.37
$R_{\nu_\mu \leftrightarrow \nu_e} \times 10^{-10}$	21.2	13.0	0.42	0.19

only 2% less events than those provided from the formalism of Refs. [44,45].

It is worth noting that, the choice of the target nucleus plays also a key role, since a light nuclear target may yield high energy recoil tails but less counts. On the contrary, a heavy nuclear target provides more counts and yields low-energy recoils making the detection more difficult. This leads to the conclusion that the best choice for a nuclear detector must consist of a combination of light and heavy nuclear isotopes [45].

3.4. New stringent limits on $\epsilon_{\mu e}^{fV}$ from $\mu^- \to e^-$ conversion

In the last part of this analysis, we exploit our channel-by-channel cross sections calculations in order to provide new limits for the NSI parameters $\epsilon_{\mu e}^{fP}$, coming out of the present and future experimental constraints of cLFV $\mu^- \to e^-$ conversion as follows. The authors of Ref. [10] (assuming that cLFV arises from loop diagrams involving virtual W's) found that the couplings of charged leptons with quarks are given by $C\epsilon_{\alpha\beta}^{fP}$, where $C \approx 0.0027$. Consequently, for the $\nu_\mu \leftrightarrow \nu_e$ transition the NSI parameters are related with the experimental upper limits of $\mu^- \to e^-$ conversion as [10]

$$\epsilon_{\mu e}^{fP} = C^{-1}\sqrt{R_{\mu e}^{(A,Z)}}. \tag{17}$$

In our calculations, up to this point we used the value $\epsilon_{\mu e}^{fV} = 2.9 \times 10^{-4}$ resulting from the PSI upper limit, $R_{\mu e}^{Ti} < 6.1 \times 10^{-13}$ [16] (occasionally, this value is a more severe constraint compared to the value $\epsilon_{\mu e}^{fV} = 7.7 \times 10^{-4}$ used in [10] which came out of the upper limit $R_{\mu e}^{Ti} < 4.3 \times 10^{-12}$ [17]).

Significantly lower upper limits on the NSI $\epsilon_{\mu e}^{fP}$ parameters of Eq. (12), are expected to be derived from the COMET, Mu2e, Mu2e at Project-X and PRIME/PRISM $\mu^- \to e^-$ conversion experiments. Then, one may compute new ratios $R_{\nu_\mu \leftrightarrow \nu_e}$ of the FC $\nu_e \leftrightarrow \nu_\mu$ reaction channel. The results for the NSI parameters $\epsilon_{\mu e}^{fV}$ and the respective ratios $R_{\nu_\mu \leftrightarrow \nu_e}$ are listed in Table 3.

Before closing we find interesting to plot the expected neutrino signals $\sigma_{\nu_\mu \to \nu_e}^{sign}(E_\nu)$ resulting by using the limits of Table 3 in two cases of ν-spectra: (i) supernova neutrinos, and (ii) laboratory neutrinos originating e.g. from the BNB (Booster Neutrino Beamline) at Fermilab known as pion decay-at-rest (DAR) neutrinos [42,43]. In the first case the simulated cross sections are obtained by employing the Supernova ν-spectra, $\eta_{\nu_\alpha}^{SN}$, discussed before [44,45] and the results are illustrated in Fig. 4(a). In the second case, the simulated cross sections are obtained by considering the laboratory neutrino distribution of the stopped pion–muon neutrinos produced according to the reactions $\pi^+ \to \mu^+ + \nu_\mu$, $\mu^+ \to e^+ + \nu_e + \tilde{\nu}_\mu$ [42,43]. In these experiments the emitted ν_e neutrino spectrum is described by the normalized distribution $\eta_{\nu_\alpha}^{lab.}$, $\alpha = e, \mu$ [35,51]. The simulated laboratory neutrino signal $\sigma_{\nu_e \to \nu_\mu}^{sign}$ is shown in Fig. 4(b).

As can be seen, in both cases the exceedingly high sensitivity of the designed experiments reduces drastically (compare Figs. 2 and 4) the area of observation of the ν-signals $\sigma_{\nu_e \to \nu_\mu}^{sign}(E_\nu)$.

We should note that for models based on non-unitary lepton mixing matrix (including seesaw), constraints on $n_{\alpha\beta}$ (related to $\epsilon_{\alpha\beta}^{fP}$ within normalisation factors [24]) may similarly come out. Obviously, for NSI considering both d and u quarks, $n_{\alpha\beta}$ enter the nuclear matrix elements of Eq. (6).

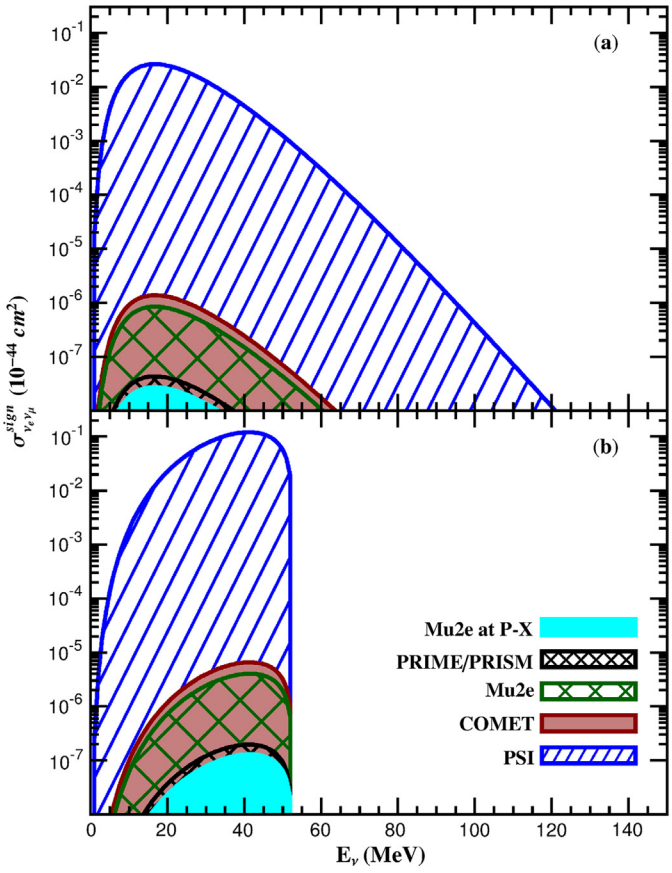

Fig. 4. Simulated ν-signal, $\sigma_{\nu_e \to \nu_\mu}^{sign}$, of the FCNC process $\nu_e + (A, Z) \to \nu_\mu + (A, Z)$ in ^{48}Ti, for the PSI and PRIME/PRISM experiments and in ^{27}Al, for the COMET, Mu2e and Mu2e at Project-X: (a) for supernova neutrinos and (b) for pion–muon stopped neutrinos. The shaded area represents the excluded region of observation by the increased sensitivity of the designed experiments. For each plot the relevant NSI parameter $\epsilon_{\mu e}^{fP}$ of Table 3 has been employed.

4. Conclusions

In conclusion, we explored NC non-standard ν-nucleus processes with realistic nuclear structure calculations. As a first step, we evaluated cross sections for the dominant coherent channel (incoming neutrino energies $0 \leqslant E_\nu \leqslant 150$ MeV, which include stopped pion–muon neutrinos, supernova neutrinos, etc). We have examined partial, integrated and total coherent cross sections and determined constraints for the ratios $R_{\nu_\alpha \to \nu_\beta}$ of all relevant reaction channels with respect to the SM cross section. Furthermore, we provided results for the differential event rates and the total number of events assuming one ton of ^{48}Ti as ν-detector material. In view of operation of the muon-to-electron conversion experiments, searching for the exotic $\mu^- \to e^-$ conversion, we concentrated on the ^{48}Ti nucleus previously used as stopping target by the PSI experiment and recently proposed to be used by the PRIME experiment at J-PARC. Similarly we have studied the ^{27}Al as ν-detector, proposed to be used as muon stopping target in the sensitive Mu2e and COMET experiments.

New stringent upper limits (up to even three orders of magnitude lower than those previously put) on the NSI (FC) parameters $\epsilon_{\mu e}^{fV}$ are extracted by using the experimental sensitivity of the $\mu^- \to e^-$ conversion experiments and our present results. By

comparing our results with those of other methods we concluded that the nuclear physics aspects (reflecting the reliability and accuracy of the cross sections), largely affect the coherent $gs \to gs$ transition rate, a result especially useful for supernova ν-detection probes and low-energy laboratory neutrinos.

Finally, we would like to remark that, $\mu^- \to e^-$ transition experiments at sensitivities down to 10^{-16}–10^{-18} have excellent capabilities to search for evidence of new physics and to study its flavour structure. These well designed experiments at Fermilab and at J-PARC, could be the starting point of such a new effort, which would complement the neutrino programs. They have significant potential for constraining the NSI parameters and shed light on FCNC processes in the leptonic sector and specifically on the existence of the charged-lepton mixing.

Acknowledgements

T.S.K. wishes to thank Robert Bernstein and Graham Kribs for the financial support to attend the Project-X Physics Study 2012 and the warm hospitality he enjoyed at Fermilab.

References

[1] Y. Kuno, Y. Okada, Rev. Mod. Phys. 73 (2001) 151.
[2] W.R. Molzon, Improved tests of muon and electron flavor symmetry in muon processes, Springer Tracts Mod. Phys. 163 (2000) 105.
[3] R.H. Bernstein, P.S. Cooper, Phys. Rep. 532 (2013) 27, arXiv:1307.5787 [hep-ex].
[4] Y.G. Cui, et al., COMET Collaboration, KEK Report 2009-10;
COMET Collaboration, The COMET Proposal to JPARC, JPARC Proposal, 2007;
A. Kurup, COMET Collaboration, Nucl. Phys. Proc. Suppl. 218 (2011) 38.
[5] Proposal to search for $\mu^- + N \to e^- + N$ with a single event sensitivity below 10^{-16}, (Mu2e Experiment) by the Mu2e Collaboration, Fermilab, October 10, 2008.
[6] R.J. Abrams, et al., Mu2e Collaboration and Project, Mu2e Conceptual Design Report, arXiv:1211.7019;
F. Cervelli, Mu2e Collaboration, J. Phys. Conf. Ser. 335 (2011) 012073.
[7] R. Bernstein, G. Kribs, Muon Physics at Project X, summary talk Project X Physics Study (PXPS12), Fermilab, June 14–28, 2012, Chicago, USA.
[8] T.S. Kosmas, Nuclear physics aspects of the exotic $\mu \to e$ conversion in nuclei, invited talk in [7].
[9] J.W.F. Valle, Nucl. Phys. B, Proc. Suppl. 229–232 (2012) 23.
[10] S. Davidson, C. Pena-Garay, N. Rius, A. Santamaria, J. High Energy Phys. 0303 (2003) 011.
[11] J. Barranco, O.G. Miranda, T.I. Rashba, J. High Energy Phys. 0512 (2005) 021.
[12] P.S. Amanik, G.M. Fuller, B. Grinstein, Astropart. Phys. 24 (2005) 160.
[13] A. Esteban-Pretel, R. Tomas, J.W.F. Valle, Phys. Rev. D 81 (2010) 063003.
[14] T.S. Kosmas, J.D. Vergados, Phys. Rep. 264 (1996) 251.
[15] F. Deppisch, T.S. Kosmas, J.W.F. Valle, Nucl. Phys. B 752 (2006) 80.
[16] P. Wintz, in: H.V. Klapdor-Kleingrothaus, I.V. Krivosheina (Eds.), Proceedings of the First International Symposium on Lepton and Baryon Number Violation, Institute of Physics Publishing, Bristol and Philadelphia, 1998, p. 534, unpublished.
[17] C. Dohmen, et al., SINDRUM-II Collaboration, Phys. Lett. B 317 (1993) 631.
[18] K. Knoepfel, et al., arXiv:1307.1168 [physics.ins-det], 2013.
[19] R.J. Barlow, Nucl. Phys. B, Proc. Suppl. 218 (2011) 44.
[20] Y. Kuno, Nucl. Phys. B, Proc. Suppl. 225 (2012) 228.
[21] J. Adam, et al., MEG Collaboration, Phys. Rev. Lett. 110 (2013) 201801.
[22] U. Bellgardt, et al., SINDRUM Collaboration, Nucl. Phys. B 299 (1988) 1.
[23] J. Schechter, J.W.F. Valle, Phys. Rev. D 22 (1980) 2227;
J. Schechter, J.W.F. Valle, Phys. Rev. D 25 (1982) 774.
[24] D.V. Forero, S. Morisi, M. Tortola, J.W.F. Valle, J. High Energy Phys. 1109 (2011) 142.
[25] S.P. Das, F.F. Deppisch, O. Kittel, J.W.F. Valle, Phys. Rev. D 86 (2012) 055006.
[26] P.S. Amanik, G.M. Fuller, Phys. Rev. D 75 (2007) 083008.
[27] A. Friedland, C. Lunardini, C. Pena-Garay, Phys. Lett. B 594 (2004) 347.
[28] A. Friedland, C. Lunardini, Phys. Rev. D 72 (2005) 053009.
[29] K. Scholberg, Phys. Rev. D 73 (2006) 033005.
[30] J. Barranco, O.G. Miranda, C.A. Moura, J.W.F. Valle, Phys. Rev. D 73 (2006) 113001.
[31] O.G. Miranda, M.A. Tortola, J.W.F. Valle, J. High Energy Phys. 0610 (2006) 008.
[32] J. Barranco, O.G. Miranda, T.I. Rashba, Phys. Rev. D 76 (2007) 073008.
[33] T.S. Kosmas, J.D. Vergados, O. Civitarese, A. Faessler, Nucl. Phys. A 570 (1994) 637.
[34] T.S. Kosmas, S. Kovalenko, I. Schmidt, Phys. Lett. B 511 (2001) 203;
T.S. Kosmas, S. Kovalenko, I. Schmidt, Phys. Lett. B 519 (2001) 78.
[35] T.S. Kosmas, E. Oset, Phys. Rev. C 53 (1996) 1409.
[36] Y. Fukuda, et al., Super-Kamiokande Collaboration, Phys. Rev. Lett. 86 (2001) 5651.
[37] Q.R. Ahmad, et al., SNO Collaboration, Phys. Rev. Lett. 89 (2002) 011302.
[38] K. Eguchi, et al., KamLAND Collaboration, Phys. Rev. Lett. 90 (2003) 021802.
[39] K. Hirata, et al., Phys. Rev. Lett. 58 (1987) 1490;
R.M. Bionta, et al., Phys. Rev. Lett. 58 (1987) 1494.
[40] M.T. Keil, G.G. Raffelt, H.-T. Janka, Astrophys. J. 590 (2003) 971.
[41] W.C. Haxton, Phys. Rev. Lett. 60 (1988) 768.
[42] A.A. Aguilar-Arevalo, et al., Phys. Rev. D 79 (2009) 072002.
[43] W.C. Louis, Prog. Part. Nucl. Phys. D 63 (2009) 51.
[44] C.J. Horowitz, K.J. Coakley, D.N. McKinsey, Phys. Rev. D 68 (2003) 023005.
[45] M. Biassoni, C. Martinez, Astropart. Phys. 36 (2012) 151.
[46] D.Z. Freedman, Phys. Rev. D 9 (1974) 1389;
A. Drukier, L. Stodolsky, Phys. Rev. D 30 (1984) 2295.
[47] Y. Giomataris, J.D. Vergados, Phys. Lett. B 634 (2006) 23.
[48] J. Monroe, P. Fisher, Phys. Rev. D 76 (2007) 033007;
A.J. Anderson, J.M. Conrad, E. Figueroa-Feliciano, K. Scholberg, J. Spitz, Phys. Rev. D 84 (2011) 013008.
[49] T.W. Donnelly, J.D. Walecka, Nucl. Phys. A 274 (1976) 368.
[50] V. Tsakstara, T.S. Kosmas, Phys. Rev. C 83 (2011) 054612.
[51] V. Tsakstara, T.S. Kosmas, Phys. Rev. C 84 (2011) 064620.
[52] H. De Vries, C.W. De Jager, C. De Vries, At. Data Nucl. Data Tables 36 (1987) 495536.
[53] D.K. Papoulias, T.S. Kosmas, Nucl. Phys. A (2013), in preparation.